Research on Variable Stiffness and Damping Magnetorheological Actuator for Robot Joint

Xiaomin Dong(✉), Weiqi Liu, Xuhong Wang, Jianqiang Yu, and Pinggen Chen

State Key Laboratory of Mechanical Transmission, Chongqing University, Chongqing, China
{xmdong, 20160713100, 20160702137, yjq2012, pgchen}@cqu.edu.cn

Abstract. Aiming at the limitation of the traditional flexible robot's single adjustment stiffness or damping, a magnetorheological (MR) actuator of which stiffness and damping can be adjusted simultaneously and independently is proposed for the robot joint. The principle of equivalent variable stiffness and damping is analyzed theoretically, and the adjustment range of stiffness and damping is deduced. As the first step, the performance of variable damping is evaluated with experiment by using a MR damper. The preliminary results show that the magnetorheological actuator is capable of changing the damping by controlling the current applied to the damper.

Keywords: Variable stiffness and damping · Flexible robot joints · Magneto-rheological fluid

1 Introduction

Rigid robots, which have been widely used in traditional industries, are scarce of flexibility. In some cases, the rigidity will cause the harmfulness for human beings [1]. Therefore, flexible robot joint is becoming more and more concerned especially to avoid injure of human being in the uncertain environment [2, 3].Early studies of flexible joints, such as the flexible joint manipulator of the German aerospace, the harmonic reducer and the torque sensor provide the factor of flexibility. However, the stiffness of the flexible joint is still very large, and the flexibility of the joint needs to be improved by a specific spring element. A solution for this problem is called *Series Elastic Actuator* (SEA) proposed by MIT leg laboratory [4]. The main feature of this method is the introduction of elastic actuators between the motor and the load. Grioli et al. [5] presented a *Variable Stiffness Actuator* (VSA). Compared with the fixed passive compliance units, the variable stiffness implementations possess the advantage of regulating stiffness and position independently and the wide range of stiffness and energy storage capabilities. However, the introduction of the variable stiffness component increases the order of the system and reduces the stability and the bandwidth [6–9]. A novel force control actuator system called *Series Damper Actuator* (SDA) [10] was proposed. It has been demonstrated that the use of physical damping in the transmission system can effectively improve its closed-loop performance [11–14].

Y. Huang et al. (Eds.): ICIRA 2017, Part III, LNAI 10464, pp. 109–119, 2017.
DOI: 10.1007/978-3-319-65298-6_11

The researches above show that the method of variable stiffness and damping is inconvenient and needs to be further improved. In the last decades, a smart damping technology, magnetorheological (MR) technology, has been received much attention due to fast response, wide damping range, reversible, low energy requirement etc. [15–18]. In our previous study [19], we proposed a linear buffering device with adaptive variable damping and stiffness based on magnetorheological, and the results had shown that the design of the buffer device and control strategy is effective. Based on the MR technology, the design of an actuator for joint of robots to realize the simultaneous adjustment of stiffness and damping was proposed in this study. This study's organization is as follows. Section 2 analyses the principle of variable stiffness and variable damping. Section 3 focuses on description of the MR damper structure design while an experiment setup is described and performance of variable stiffness are presented in Sect. 4. The conclusions and future work are addressed in Sect. 5.

2 Analysis of Variable Stiffness and Variable Damping

In this paper, the variable stiffness and damping actuator, which consists of two magnetorheological damper c_1, c_2 and two torsional springs k_{s1}, k_{s2}, can achieve real-time damping and stiffness changes. As can be seen in Fig. 1(a), the magnetorheological damper c_2 and the torsion spring k_{s2} are connected in parallel to form a unit which is connected in series with the torsion spring k_{s1} and then in parallel with the magnetorheological damper c_1. Figure 1(b) shows the equivalent model of the joint, which has the equivalent damping coefficient c_s and the equivalent stiffness k_s.

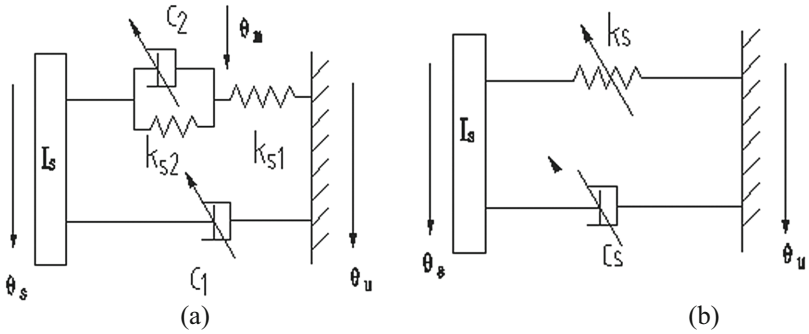

Fig. 1. Joint model of variable stiffness and damping and its equivalent model

When the rotary axis moves, the magnetorheological fluid generates damping at the gap between the shaft and the outer cylinder. The rheological properties of the MR fluid will change with the change of the applied magnetic field. After theoretical deduction and pre-analysis of the working characteristics of magnetorheological damper, the relationship between the damping force F_d, the relative speed of the shaft v and the applied current I can be expressed as [20]:

$$F_d = c_0 v + F_{MR} \operatorname{sgn} v \tag{1}$$

$$F_{MR} = aI^2 + bI + c \tag{2}$$

Where c_0 is viscous damping coefficient, F_{MR} is coulomb damping force; a,b,c are constants obtained by fitting the test data.

Equation (1) shows that the damping force of the magnetorheological damper is composed of viscous damping force and Coulomb damping force. When the geometrical dimension of the damper is determined, the viscous damping force is only a function of the velocity of the piston. The Coulomb damping force is a function of the applied current, so it is possible to adjust the damping force by adjusting the magnitude of the applied current of the damper to realize the change of the damping coefficient.

According to Newton's second law, the dynamic equation of Fig. 1(a) is obtained:

$$I_s\ddot{\theta}_s - c_1\left(\dot{\theta}_s - \dot{\theta}_u\right) - k_{s2}(\theta_s - \theta_m) - c_2\left(\dot{\theta}_s - \dot{\theta}_m\right) = 0 \tag{3}$$

$$I_u\ddot{\theta}_u + c_1\left(\dot{\theta}_u - \dot{\theta}_s\right) + k_{s1}(\theta_u - \theta_m) = 0 \tag{4}$$

$$k_{s2}(\theta_s - \theta_m) + c_2\left(\dot{\theta}_s - \dot{\theta}_m\right) - k_{s1}(\theta_m - \theta_u) = 0 \tag{5}$$

The dynamic equation of Fig. 1(b) is obtained:

$$I_s\ddot{\theta}_s - c_s\left(\dot{\theta}_s - \dot{\theta}_u\right) - k_s(\theta_s - \theta_u) = 0 \tag{6}$$

$$I_u\ddot{\theta}_u + c_s\left(\dot{\theta}_s - \dot{\theta}_u\right) + k_s(\theta_s - \theta_u) = 0 \tag{7}$$

where I_s is the moment of inertia of the output shaft, θ_s is the turning angles of the output shaft, c_1 and c_2 are the damping coefficients of the two dampers, respectively, θ_m is the turning angles of the middle shaft, θ_u is the excitation of the joint.

Using the Laplace transform, we can get the transfer function between the output shaft angle and the input corner excitation of Fig. 1(a):

$$\frac{\theta_s(s)}{\theta_u(s)} = \frac{k_{s1} - k_{s1}^2(k_{s1}+k_{s2})/\left[(k_{s1}+k_{s2})^2 - c_2^2 s^2\right] + \left\{c_1 + k_{s1} - k^2/\left[(k_{s1}+k_{s2})^2 - c_2^2 w^2\right]\right\}s}{I_s s^2 + k_{s1} - k_{s1}^2(k_{s1}+k_{s2})/\left[(k_{s1}+k_{s2})^2 - c_2^2 s^2\right] + \left\{c_1 + k_{s1} - k^2/\left[(k_{s1}+k_{s2})^2 - c_2^2 s^2\right]\right\}s} \tag{8}$$

From Fig. 1(b) we can get the equivalent transfer function as:

$$\frac{\theta_s(s)}{\theta_u(s)} = \frac{k_s + c_s s}{I_s s^2 + k_s + c_s s} \tag{9}$$

The $s = jw$, w is the excitation frequency, into the Formulas (8) and (9).Then we can get:

$$\frac{\theta_s(jw)}{\theta_u(jw)} = \frac{k_{s1} - k_{s1}^2(k_{s1}+k_{s2})/\left[(k_{s1}+k_{s2})^2 + c_2^2w^2\right] + \left\{c_1 + k_{s1}^2c_2/\left[(k_{s1}+k_{s2})^2 + c_2^2w^2\right]\right\}jw}{-I_sw^2 + k_{s1} - k_{s1}^2(k_{s1}+k_{s2})/\left[(k_{s1}+k_{s2})^2 + c_2^2w^2\right] + \left\{c_1 + k_{s1}^2c_2/\left[(k_{s1}+k_{s2})^2 + c_2^2w^2\right]\right\}jw} \tag{10}$$

$$\frac{\theta_s(jw)}{\theta_u(jw)} = \frac{k_s + c_sjw}{-I_sw^2 + k_s + c_sjw} \tag{11}$$

Contrast Formulas (10) and (11) can be introduced:

$$c_s = c_1 + \frac{k_{s1}^2c_2}{(k_{s1}+k_{s2})^2 + c_2^2w^2} = c_1 + \frac{1}{\frac{(1+\eta)^2}{c_2} + c_2\left(\frac{w}{k_{s1}}\right)^2} \tag{12}$$

$$k_s = k_{s1} - \frac{k_{s1}^2(k_{s1}+k_{s2})}{(k_{s1}+k_{s2})^2 + c_2^2w^2} = k_{s1}\left[1 - \frac{1+\eta}{(1+\eta)^2 + \left(\frac{c_2w}{k_{s1}}\right)^2}\right] \tag{13}$$

Where η is the spring stiffness ratio,$\eta = \frac{k_{s2}}{k_{s1}}$,$w$ is the excitation frequency. And $\xi_1 = \frac{c_1}{2\sqrt{I_sk_{s1}}}$, $\xi_2 = \frac{c_2}{2\sqrt{I_sk_{s2}}}$, ξ_1, ξ_2 are the damping ratios of two dampers, respectively,.

When the excitation frequency w is constant, the Eqs. (12) and (13) are discussed as follows:

- The equivalent stiffness k_s of Fig. 1(b) is independent of the damping coefficient c_1; the equivalent stiffness k_s and the equivalent damping coefficient c_s have nonlinear function relationship with the damping coefficient c_2.
- Formula (12) shows that when c_2 is equal to zero or infinity, $c_s = c_1$; When c_2 increases from zero to infinity, the c_s will firstly increase and then decrease on, c_1 but it is always greater than c_1.
- Formula (13) shows that, when $c_2 = 0$, $k_s = \frac{k_{s1}\cdot k_{s2}}{k_{s1}+k_{s2}}$, equivalent to two springs in series. When $c_2 = \infty$, then $k_s = k_{s1}$.

From the above discussion, when the damper damping coefficient is adjusted, the equivalent damping and stiffness of the system will change at the same time. As a result, the equivalently variable stiffness range is $\left[\frac{k_{s1}\cdot k_{s2}}{k_{s1}+k_{s2}}, k_{s1}\right]$.

Assuming $I_s = 3.75 \times 10^{-5}kg.m^2$, $k_{s1} = 0.2N.m/rad$, $\xi_1 = 0.01$, when giving ξ_2 different values, the frequency response characteristics of the system as shown in Fig. 2.

As can be seen from Fig. 2, with the damping ratio ξ_2 increasing, the resonance peak will shift to high frequency domain, which means that the equivalent stiffness will be increased.

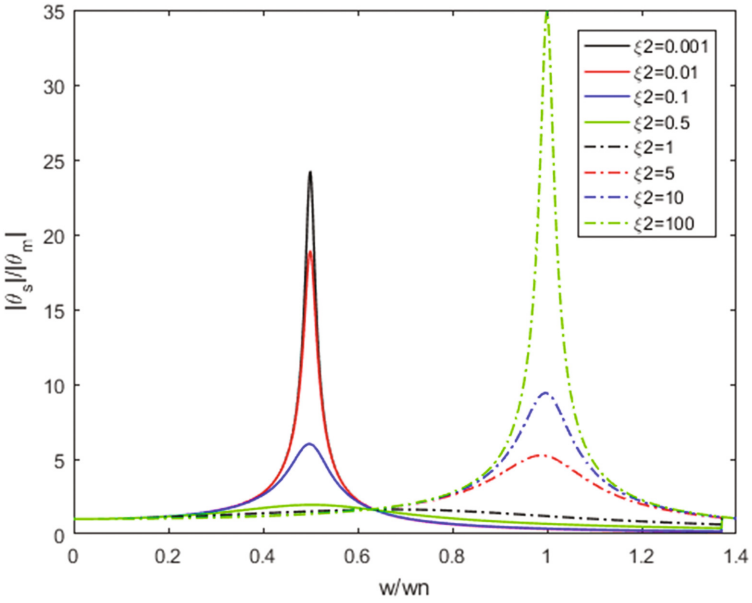

Fig. 2. The frequency response characteristics of the system

3 Structural Design of Magnetorheological Damper

To implement the variable stiffness and damping, the ability of variable damping is investigated firstly. A rotary MR damper is designed in Fig. 3. The damper consists of the outer cylinder, the iron core and the coil. In order to improve the magnetic field strength of the working area, the coil is designed as a double coil structure. The two-stage excitation coil is wound around the core through the center hole of the left end cap, and the size of the magnetic field can be changed by changing the current. The core and outer cylinder are positioned by bearings and fitted with O-rings to prevent leakage of magneto-rheological fluids. When the rotary axis moves, the magnetorheological fluid generates damping at the gap between the iron core and the outer cylinder.

Magnetic field analysis is an important part in the design of MR damper. It is necessary to simplify the structure of the damper when the finite element method is used to analyze the magnetic field. The structure and calculation model of the magnetic circuit can be simplified effectively by eliminating the components of the damper such as bearings and O-ring seals. In order to improve the computational efficiency of ANSYS calculation, the calculated model chooses the simplified 2-D axisymmetric model. The finite element model of the MR damper is shown in Fig. 4. The different areas are given the magnetic properties of the respective corresponding materials The current density applied to the magnetic field strength generated by the coil can be approximated by Eq. (14).

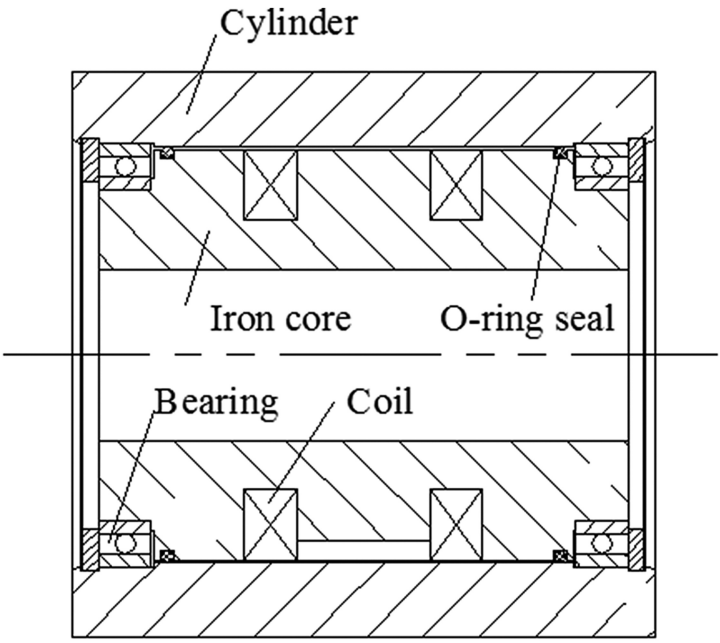

Fig. 3. The structure of MR damper

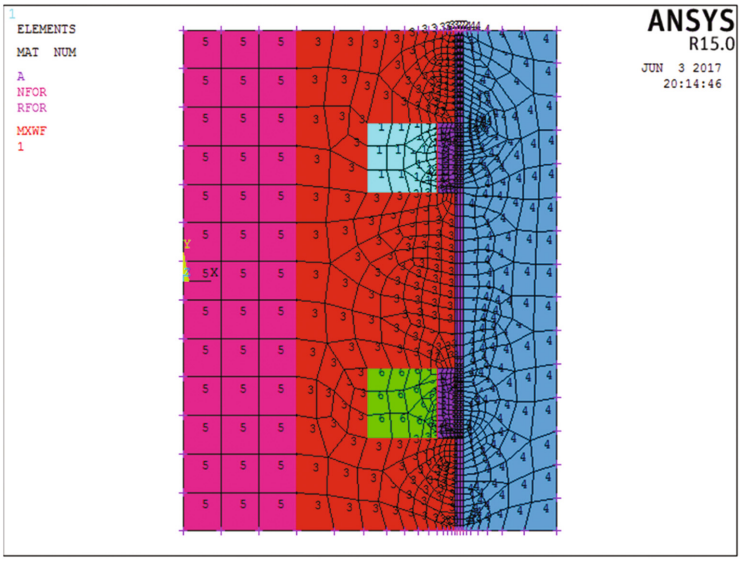

Fig. 4. The finite element model of the MR damper

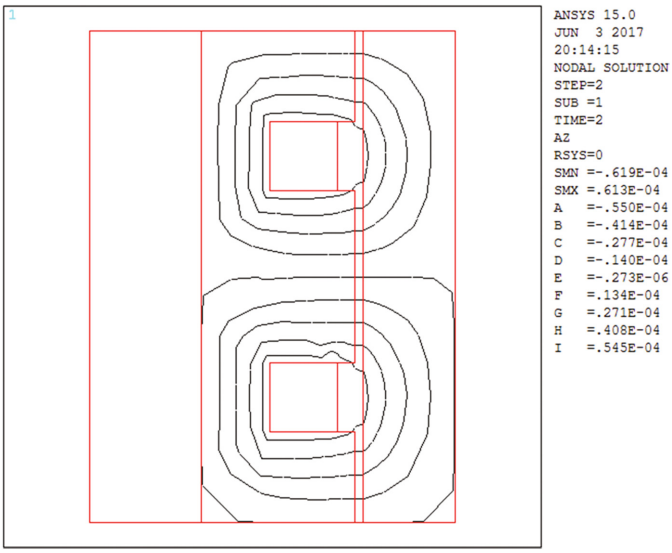

Fig. 5. Magnetic field distribution of damper

$$J = NI/A \tag{14}$$

Where N is the number of turns of the coil, I is the current size, and A is the cross-sectional area of the coil groove.

Through the previous steps, ANSYS calculated magnetic field distribution of damper shown in Fig. 5, the magnetic flux density of the distribution shown in Fig. 6.

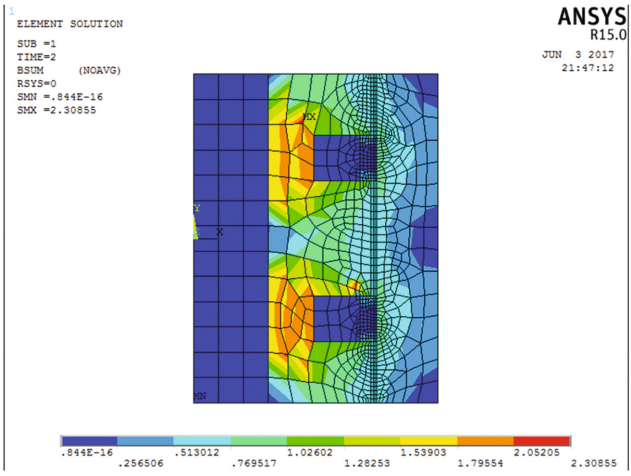

Fig. 6. The magnetic flux density of the distribution

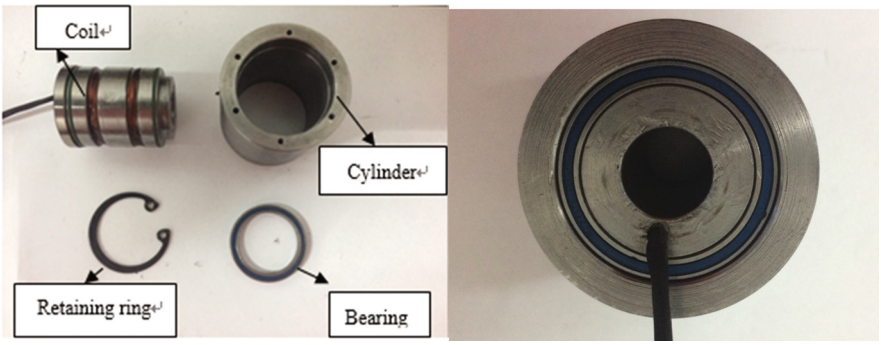

Fig. 7. Parts and assembly drawings of MR damper

The finished parts and assembly drawings are shown in Fig. 7. After the MR damper is assembled, the damper is tested preliminarily. The geometrical parameters of the MR damper are given in Table 1.

Table 1. Parameters of rotary MR damper

Parameter	Value
Gap	2 mm
Total length	44 mm
Working diameter	31 mm
Maximum diameter	42.7 mm
The number of turns of the coil	85
The resistance of the coil	2.5 Ω
The volume of MR fluid	3 mL

4 Experimental Evaluation of Variable Damping

In this section, a one-way rotation test of a rotary MR damper is designed to test the relationship between the damping torque, the current and speed, in order to verify the variable damping characteristics of actuator.

As shown in Fig. 8, the test system consists of a console, two couplings, a variable speed motor, a torque sensor, a rotary MR damper and a DC power. MR damper weighs about 400 g. At the beginning of the test, the current is set to a constant. Under the same current, the motor speed will change continuously from 0 rpm to 180 rpm.

The results of the test are shown in Fig. 9. The dashed lines and the dotted lines respectively represent the experimental results and the theoretical results.

From Fig. 9, it can be seen that the damping torque will increase with the increment of current. Compared to current input, the rotational speed has little effect on the performance of output damping torque. The reason may be that the increased temperature reduces the performance of MR fluid. On the other hand, this provides the good controllability. According to the test result, the obtained maximum damping

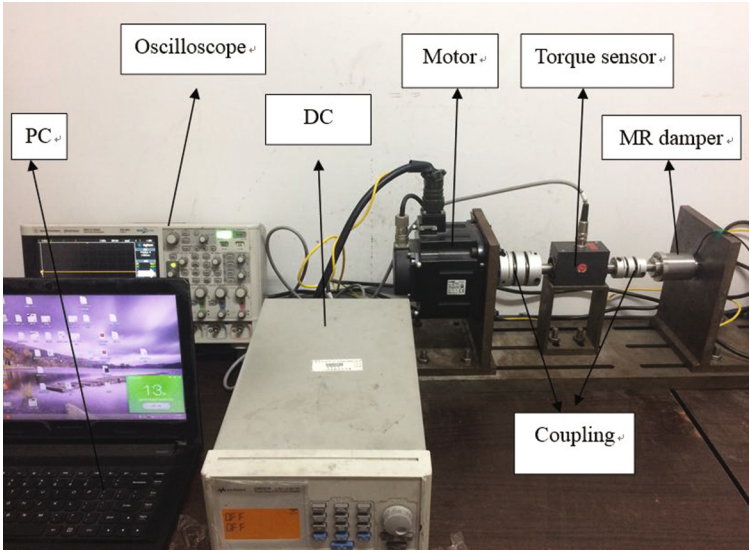

Fig. 8. The test system rotary MR damper

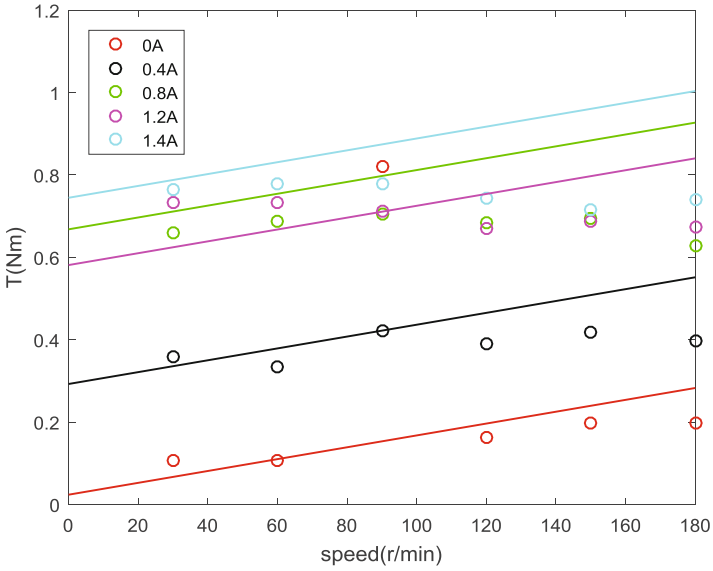

Fig. 9. Comparison of experimental and theoretical

torque is around 0.78 Nm under the current of 1.4 A. The viscous damping torque T_η of the damper is the damping torque in the case of a current of 0 A while the maximum damping torque T_{total} is the damping torque measured at a current of 1.4 A. The adjustable range D of damper damping is:

$$D = \frac{T_{total}}{T_\eta} = \frac{0.78}{0.1} = 7.8 \tag{15}$$

5 Conclusions and Future Work

A variable stiffness and damping MR actuator for robot joint is investigated. The variable stiffness characteristics are analyzed. As the first step, a rotary MR damper is developed to implement the variable damping feature. The obtained maximum damping torque reaches to 0.78 Nm. In addition, the damping dynamic range is 7.8. The variable stiffness feature will be investigated in the near future.

Acknowledgments. We would like to thank the authors of the references for their enlightenment. This research is also supported financially by the National Natural Science Foundation of People's Republic of China (Project No. 51275539 and 51675063), the Chongqing University Postgraduates' Innovation Project (No. CYB15017). These supports are gratefully acknowledged.

References

1. Vanderborght, B., Albu-Schaeffer, A., Bicchi, A.: Variable impedance actuators: A review. Robot. Auton. Syst. **61**(12), 1601–1614 (2013)
2. Visser, L.C., Carloni, R., Stramigioli, S.: Energy-efficient variable stiffness actuators. IEEE Trans. Robot. **27**, 865–875 (2011). IEEE Press
3. Bigge, B., Harvey, I.R.: Programmable springs: developing actuators with programmable compliance for autonomous robots. Robot. J. Auton. Syst. **55**(9), 728–734 (2007)
4. Robinson, D.W., Pratt, J.E., Paluska, D.J., et al.: Series elastic actuator development for a biomimetic walking robot. In: IEEE/ASME International Conference on Advanced Intelligent Mechatronics, Proceedings, pp. 561–568. IEEE Xplore (1999)
5. Grioli, G., Garabini, M., Catalano, M., et al.: Variable stiffness actuators: the user's point of view. IEEE Robot. Autom. Mag. (under review)
6. Laffranchi, M., Tsagarakis, N.G., Caldwell, D.G.: Analysis and development of a semiactive damper for compliant actuation systems. IEEE/ASME Trans. Mechatron. **18**(2), 744–753 (2013)
7. Laffranchi, M., Tsagarakis, N., Caldwell, D.G.: A compact compliant actuator (CompAct™) with variable physical damping. In: EEE International Conference on Robotics and Automation, pp. 4644–4650. IEEE Xplore(2011)
8. Laffranchi, M., Tsagarakis, N.G., Caldwell, D.G.: A variable physical damping actuator (VPDA) for compliant robotic joints. In: IEEE International Conference on Robotics and Automation, pp. 1668–1674. IEEE Xplore(2010)

9. Hurst, J.W., Rizzi, A.A., Hobbelen, D.: Series elastic actuation: potential and pitfalls. In: International Conference on Climbing and Walking Robots (2004)
10. Chew, C.M., Hong, G.S., Zhou, W.: Series damper actuator: a novel force/torque control actuator. In: IEEE/RAS International Conference on Humanoid Robots, pp. 533–546. IEEE Xplore(2004)
11. Garcia, E., Arevalo, J.C., Muñoz, G., et al.: Combining series elastic actuation and magneto-rheological damping for the control of agile locomotion. Robot. Auton. Syst. **59** (10), 827–839 (2011)
12. Radulescu, A., Howard, M., Braun, D. J., Vijayakumar, S.: Exploiting variable physical damping in rapid movement tasks. In: 2012 IEEE/ASME International Conference on Advanced Intelligent Mechatronics (AIM), pp. 141–148. IEEE, Taiwan (2012)
13. Enoch, A., Sutas, A., Nakaoka, S.I., Vijayakumar, S.: Blue: A bipedal robot with variable stiffness and damping. In: 2012 12th IEEE-RAS International Conference on Humanoid Robots (Humanoids), pp. 487–494. IEEE (2012)
14. Roy, N., Newman, P., Srinivasa, S.: CompAct™ Arm: a Compliant Manipulator with Intrinsic Variable Physical Damping. MIT Press (2012)
15. Imaduddin, F., Mazlan, S.A., Zamzuri, H.: A design and modelling review of rotary magnetorheological damper. Mater. Des. **51**(5), 575–591 (2013)
16. Jiménezfabián, R., Verlinden, O.: Review of control algorithms for robotic ankle systems in lower-limb orthoses, prostheses, and exoskeletons. **34**(4), 397–408 (2011)
17. Yu, J., Dong, X., Wang, W.: Prototype and test of a novel rotary magnetorheological damper based on helical flow. Smart Mater. Struct. **25**(2), 025006 (2016)
18. Chen, J., Liao, W.H.: Design and control of a Magnetorheological actuator for leg exoskeleton. In: International Conference on Robotics and Biomimetics, pp. 1388–1393. IEEE (2007)
19. Dong, X., Yu, M.: Absorbing control of magneto-rheological variable stiffness and damping system under impact load. Trans. Chin. Soc. Agric. Mach. (2010)
20. Yu, M., Liao, C., Chen, W., Huang, S.: Research on control method for MR damper. Chin. J. Chem. Phys. (2001) (in Chinese)